Polymer Journal (2012) 44, 181–188

www.nature.com/pj

ORIGINAL ARTICLE

pH-responsive flocculation and dispersion behavior of Janus particles in water

Masanori Ito[1], Ryusuke Enomoto[1], Kazuki Osawa[1], Yusuke Daiko[1], Tetsuo Yazawa[1], Syuji Fujii[2], Yuichi Yokoyama[2], Yuki Miyanari[2], Yoshinobu Nakamura[2], Aiko Nakao[3], Yasuhiko Iwasaki[4] and Shin-ichi Yusa[1]

Gold was vacuum-deposited on one side of 6-μm-diameter SiO_2 particles to prepare Janus particles (JPs). A thiol-terminated pH-responsive polymer (pAaH-SH), prepared via reversible addition–fragmentation chain transfer (RAFT) -controlled radical polymerization, was immobilized on the gold surface of the JPs as confirmed by attenuated total reflection-Fourier transform infrared and X-ray photoelectron spectroscopy measurement techniques. A fluorescein-labeled polymer (p(AaH/Flu)-SH) was also prepared via RAFT, and immobilization of p(AaH/Flu)-SH only on the gold surface of the JPs was confirmed by fluorescence microscopy observations. The flocculation and dispersion behavior of pAaH-SH-grafted JPs was observed with an optical microscope and was found to be varied with the solution pH.
Polymer Journal (2012) **44,** 181–188; doi:10.1038/pj.2011.94; published online 2 November 2011

Keywords: controlled radical polymerization; graft; Janus particles; pH-responsive polymer

INTRODUCTION

Particles, ranging from nanometer to micrometer sizes, have been investigated for many applications such as engineering products and biomaterials. When particles are used in advanced materials, the control of their shape, size and composition is important to confer high functionality. Shape-controlled particles—Janus particles (JPs),[1–9] whose two sides show different properties such as differences in charge,[10] polarity[11] or optical and magnetic properties[12]—are unique among micro- and nano-particles. JPs have a demonstrated potential for use in functional emulsifying agents,[13] in electronic paper,[14] and as agents for the delivery and controlled release of drugs.[15]

Several methods of preparing JPs are known.[16,17] Feng *et al.*[18] reported the preparation of a Janus-type dendrimer-like polymer using 3-allyloxy-1,2-propanediol as a latent AB_2-type heterofunctional initiator for anionic ring-opening polymerization of ethylene oxide together with 2-(3′-chloromethylbenzyloxymethyl)-2-methyl-5,5-dimethyl-1,3-dioxane as a selective branching agent for the poly (ethylene oxide) chain ends. An alternative synthesis route uses inorganic colloid templates, such as SiO_2, with half of the template surface modified. Love *et al.*[19] prepared nanometer-size JPs, consisting of SiO_2, half-coated with metal, by forming monolayers or multilayers of silica colloidal crystals on glass substrates and coating them with a thin film of metal, such as gold or palladium, by physical vapor deposition. These studies motivated us to synthesize hybrid JPs composed of inorganic SiO_2 particles covered on one side with gold, onto which pH-responsive polymers were immobilized.

Polymer synthesis methods involving controlled/living radical polymerization, such as atom transfer radical polymerization[20] or reversible addition-fragmentation chain transfer (RAFT)[21] polymerization, have been used to prepare specialty polymers for various applications. RAFT radical polymerization uses a similar method to conventional radical polymerization, except for the addition of a dithioester group containing a chain transfer agent. Polymers synthesized via RAFT radical polymerization contain a dithioester group at the polymer chain end, and can therefore be converted to thiol-terminated polymers by hydrolysis.[22,23]

In this paper, we report the synthesis of JPs composed of SiO_2 particles with gold particles sputtered onto one side. Sodium 6-acrylamidohexanoate (AaH) was polymerized via RAFT-controlled radical polymerization (Figure 1). The resultant poly(sodium 6-acrylamidohexanoate) (pAaH) has a dithioester group at the polymer chain end, which can be converted to pAaH with a thiol group at the polymer chain end (pAaH-SH) by hydrolysis. The pAaH polymer can dissolve in water at a pH higher than 5.5, but it is precipitated from water at a pH below 5.5, owing to protonation of the pendant carboxyl groups. X-ray photoelectron spectroscopy (XPS), contact angle measurements, and attenuated total reflection-Fourier transform infrared (ATR-FTIR) were used to confirm that pAaH with a terminal thiol

[1]Department of Materials Science and Chemistry, University of Hyogo, Himeji, Hyogo, Japan; [2]Department of Applied Chemistry, Faculty of Engineering, Osaka Institute of Technology, Asahi-ku, Osaka, Japan; [3]Beam Application Team, Discovery Research Institute, RIKEN, Wako, Saitama, Japan and [4]Department of Chemistry and Materials Engineering, Faculty of Chemistry, Materials and Bioengineering, Kansai University, Suita-shi, Osaka, Japan
Correspondence: Dr S Yusa, Department of Materials Science and Chemistry, University of Hyogo, 2167 Shosha, Himeji, Hyogo 671-2280, Japan.
E-mail: yusa@eng.u-hyogo.ac.jp
Received 7 July 2011; revised 15 August 2011; accepted 18 August 2011; published online 2 November 2011

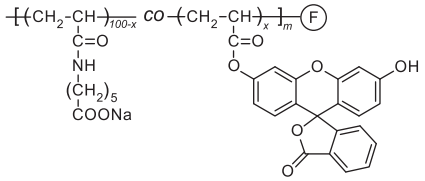

	x (mol%)	*m*	Ⓕ
pAaH	0	220	
pAaH-SH	0	220	
p(AaH/Flu)	0.2	180	
p(AaH/Flu)-SH	0.2	180	
conventional p(AaH/Flu)	0.1	8784	—

Figure 1 Chemical structures of pH-responsive polymers.

group was immobilized onto the gold surface. Fluorescein-labeled pAaH (p(AaH/Flu)-SH) was also prepared via RAFT, and it was confirmed by fluorescence microscopy observation that p(AaH/Flu)-SH was immobilized only onto the gold surface of the JPs. The pH-responsive association and dissociation behavior of pAaH-grafted JPs (pAaH-JPs) in water was elucidated using optical microscopy.

EXPERIMENTAL PROCEDURES

Materials

SiO_2 particles 6 μm in diameter (Hipresica FQ) were donated by Ube-Nitto Kasei (Tokyo, Japan). Sodium 6-acrylamidohexanoate (AaH)[24] and 4-cyanopentanoic acid dithiobenzoate[25] were synthesized, as reported previously. 2,2′-Azobis(isobutyronitrile) (>98%, AIBN) from Wako Pure Chemical Industries (Osaka, Japan) was recrystallized from methanol. Methanol was dried over 4 Å molecular sieves and purified by distillation. Sodium borohydride (98%, $NaBH_4$), from Kanto Chemical (Tokyo, Japan), and fluorescein *O*-acrylate (97%, Flu), from Sigma Aldrich (St Louis, MO, USA), were used without further purification. Water was purified using a Millipore (Billerica, MA, USA) Milli-Q system.

Preparation of Thiol-terminated Poly(sodium 6-acrylamidohexanoate) (pAaH-SH) by RAFT Polymerization

AaH (10.0 g, 53.0 mmol), 4-cyanopentanoic acid dithiobenzoate (50.0 mg, 0.179 mmol), and AIBN (12.0 mg, 0.0731 mmol) were dissolved in 27 ml of methanol. The solution was deoxygenated by purging with Ar gas for 30 min. Polymerization was carried out at 60 °C for 24 h. After polymerization, a portion of the solution was removed to estimate the extent of conversion by ^{1}H NMR. The polymer was purified by reprecipitating twice from methanol into a large excess of diethyl ether. The precipitate was dissolved in water; the solution was then dialyzed against a pH 10 aqueous solution for 2 days and against pure water for 1 day. Poly(sodium 6-acrylamidohexanoate) (pAaH) was recovered by a freeze-drying technique in the form of a pink powder (7.40 g, 73.6%). ^{1}H NMR indicated that the conversion was 85.7%, and the degree of polymerization for pAaH was estimated at 220 on the basis of the conversion. The number-average molecular weight (M_n) and molecular weight distribution (M_w/M_n) for pAaH were estimated by gel-permeation chromatography (GPC) to be 4.93×10^4 and 1.19, respectively.

The dithioester group at one end of the polymer chain was cleaved by reduction using $NaBH_4$. Poly(sodium 6-acrylamidohexanoate) (500 mg, 8.85×10^{-3} mmol, M_n(GPC)=4.93×10^4, M_w/M_n=1.19) was dissolved in 10 ml of methanol. $NaBH_4$ (6.6 mg, 0.177 mmol) was added, and the solution was stirred for 2 h at room temperature. Purification was performed by dialysis against a pH-10 aqueous solution for 2 days, and against pure water for 1 day. Thiol-terminated pAaH (pAaH-SH) was recovered by a freeze-drying technique as a white powder (320 mg, 64.0%). The M_n and M_w/M_n values were estimated by GPC to be 4.96×10^4 and 1.20, respectively.

Synthesis of fluorescein-labeled pAaH-SH (p(AaH/Flu)-SH) by RAFT polymerization

AaH (3.00 g, 0.0145 mol), Flu (9.32 mg, 0.0241 mmol), AIBN (4.0 mg, 0.0244 mmol), and 4-cyanopentanoic acid dithiobenzoate (13.5 mg, 0.0483 mmol) were dissolved in 14 ml of methanol. The solution was deoxygenated by purging with Ar gas for 30 min, and polymerization was carried out at 60 °C for 24 h. After polymerization, a portion of the solution was removed to estimate the extent of conversion by ^{1}H NMR. The polymer was purified by reprecipitating twice from methanol into a large excess of diethyl ether. The resultant fluorescein-labeled polymer (p(AaH/Flu)) was dried at 60 °C in a vacuum oven and obtained as a pale yellow powder (1.72 g, 57.2%). ^{1}H NMR analysis indicated that the conversion was 60.1%, and the degree of polymerization for p(AaH/Flu) was estimated at 180 on the basis of the conversion. The M_n and M_w/M_n values were estimated by GPC to be 3.50×10^4 and 1.05, respectively. The dithioester group at one end of the polymer chain was cleaved in a similar manner to the equivalent process for the preparation of pAaH-SH. The M_n and M_w/M_n values of the resultant polymer (p(AaH/Flu)-SH) were estimated by GPC to be 3.42×10^4 and 1.05, respectively. The Flu content in p(AaH/Flu)-SH, determined from ultraviolet (UV)–visible absorption spectra in methanol, was 0.2 mol%.

Synthesis of fluorescein-labeled pAaH by conventional free radical polymerization (Conventional p(AaH/Flu))

AaH (3.00 g, 0.0145 mol), Flu (9.32 mg, 0.0241 mmol), and AIBN (4.0 mg, 0.0244 mmol) were dissolved in 14 ml of methanol. The solution was deoxygenated by purging with Ar gas for 30 min, and polymerization was carried out at 60 °C for 24 h. The resultant polymer was purified in a similar manner to pAaH, and fluorescein-labeled pAaH (conventional p(AaH/Flu)) was obtained as a white powder (1.72 g, 57.2%). The M_n and M_w/M_n values for conventional p(AaH/Flu) were estimated by GPC to be 1.82×10^6 and 1.42, respectively. The degree of polymerization for conventional p(AaH/Flu) was estimated at 8 784 on the basis of GPC measurements. The Flu content in p(AaH/Flu), determined from UV–visible absorption spectra in methanol solution, was 0.1 mol %.

Synthesis of pAaH-SH-grafted Gold-sputtered cover glass

Gold was deposited on a microscope slide cover glass by vacuum deposition using a Sanyu Electron (Tokyo, Japan) Super-mini SVC-700 vacuum coater equipped with an Inficon (Bad Ragaz, Switzerland) SQM-160 rate/thickness monitor. The thickness of the gold layer on the slide glass was set to be 100 nm, and the gold covered the slide glass completely as confirmed by XPS study. The polymer concentration (C_p) of pAaH-SH in pure water was adjusted to 10 g l^{-1}. The aqueous polymer solution (200 mg) was dropped onto the gold-sputtered cover glass over a range of 15×15 mm. The gold surface was washed with pure water, and the water was blotted with filter paper to remove excess polymer. Water adjusted to pH 3 or 10 was dropped onto the gold surface to control the degree of protonation of the pendant carboxyl groups in pAaH, and the water was blotted with filter paper.

Synthesis of JPs of silica half-coated with gold

SiO_2 particles half-coated with gold (JPs) were synthesized according to a previously reported method.[26] A typical procedure for the synthesis is shown in Figure 2. Distilled water (3.2 ml) was placed on a glass substrate (76×26 mm), and then SiO_2 particles (0.5 g) dispersed in 1-butanol (5.56 ml) was poured onto the air–water surface prepared on the glass substrate. The system was left for 3 days to allow the water and 1-butanol to evaporate completely, which left a 2D silica colloidal crystal monolayer on the glass substrate. Gold was deposited on the 2D colloidal crystal layer by vacuum deposition. The thickness of the gold layer was kept at 100 nm on the surface of the SiO_2 particles. The JPs

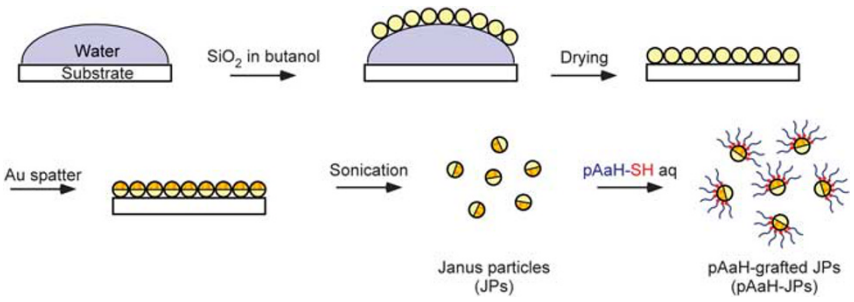

Figure 2 Synthesis route of pAaH-JPs.

were released from the glass substrate surface by sonication in pure water. The concentration of JPs dispersed in water was found to be 0.2 wt %.

Immobilization of the polymers on JPs

A typical procedure for immobilization of pAaH-SH on the JP surface is as follows: An aqueous solution of the polymer (10 g l^{-1}, 10 ml) was mixed with water-dispersed JPs (0.2 wt %, 4.2 ml), and the solution was stirred for 24 h at room temperature. After the reaction, pAaH-JPs were washed by centrifugation at 13 300 rpm for 10 min using pure water (twice). The concentration of pAaH-JPs was adjusted to 0.58 wt % by adding pure water.

p(AaH/Flu)-SH was immobilized on the surface of JPs using the same method as described for pAaH-JPs. In a reference experiment, conventional p(AaH/Flu), without thiol groups, was mixed with JPs in water; the JPs were then washed with pure water and observed under optical and fluorescence microscopes.

Measurements

UV–visible absorption. UV–visible absorption spectra and percent transmittance (%*T*) at 600 nm were measured using a JASCO (Tokyo, Japan) V-530 UV/VIS spectrophotometer.

^{1}H NMR. ^{1}H NMR spectra were obtained using a Bruker BioSpin (Billerica, MA, USA) DRX 500 FT-NMR spectrometer at 500 MHz.

Gel permeation chromatography. GPC measurements for polymer samples were performed using a refractive index detector equipped with a Shodex (Tokyo, Japan) 7.0-μm bead size GF-7 M HQ column (exclusion limit $\sim 10^7$) working at 40 °C with a flow rate of 0.6 ml/min. Phosphate buffer (pH 8, 50 mM) containing 9.1 vol % acetonitrile was used as an eluent. The values of M_n and M_w/M_n were calibrated using standard sodium poly(styrenesulfonate) samples of 11 different molecular weights ranging from 1.37×10^3 to 2.16×10^6.

Scanning electron microscope. The fine structure of JPs was observed using a Keyence (Tokyo, Japan) VE-9800 at 12 kV. Samples for scanning electron microscopy were prepared by directly depositing one drop of water containing dispersed JPs onto electrically conductive tape and then drying the sample under vacuum. The samples were treated with Pt sputtering using a Sanyu Electron (Tokyo, Japan) Quick Coater Sc-701 MKII.

Optical and fluorescence microscopy. Optical and fluorescence micrographs were obtained using a Keyence (Tokyo, Japan) Biorevo BZ-8000 equipped with a Nikon (Tokyo, Japan) FL ELWD ADM 20×C objective lens (excitation/emission 480 nm/510 nm).

X-ray photoelectron spectroscopy. Elemental quantification and chemical characterization of gold-sputtered slide glasses were obtained by XPS analysis using a Thermo Fischer Scientific Inc. (Waltham, USA) ESCALab 250 spectrometer employing monochromatic AlK X-ray radiation (1486.6 eV). The system was operated at 15 kV and 200 W. The base pressure of the analysis chamber was less than 10^{-8} Pa. Standardization was achieved using the C1 transition (284.8 eV). Background removal was carried out using a Thermo Fischer Scientific Inc. advantage analysis software package.

Contact angle. The contact angles of the gold surface were measured by a sessile drop technique using Drop Master 300 (Kyowa Interface Science, Saitama, Japan). A 1.0-μl drop of pure water was carefully placed on meticulously dried portions of the pAaH-SH-grafted gold-sputtered slide glass using a micropipette. The image of the drop on the surface was captured within 5 seconds of drop deposition to minimize error due to evaporation. All measurements were repeated on at least five dried areas of the gold surface to determine reproducibility.

Attenuated total reflection Fourier transform infrared. ATR-FTIR spectra were obtained using a JASCO (Tokyo, Japan) FT/IR-4200 spectrophotometer with an ATR PRO450-S base kit and a ZnSe prism. Spectra were collected over 64 scans with a spectral resolution of 1.0 cm^{-1}.

Thermo gravimetric analysis. Thermo gravimetric analysis (TGA) measurements were carried out using an Exstar TG/DTA 6200 apparatus (SII Technology Inc., Chiba, Japan) under nitrogen with a flow rate of 100 ml min^{-1}. Samples were heated from 25 to 800 °C at 5 °C per min. The graft density of pAaH-SH (Γ, chains/nm^2) can be estimated by TGA as follows:

$$\Gamma=\frac{(W_{pAaH}/100-W_{pAaH})\times(S_{Au}\times L_{Au}\times\rho_{Au}+V_{SiO_2}\times\rho_{SiO_2})\times N_A}{M_{pAaH}\times S_{Au}} \quad (1)$$

Here, W_{pAaH} is the percent weight loss corresponding to the decomposition of the pAaH-SH chains; S_{Au} is the specific surface area of gold, that is, half the surface area of SiO_2 particles calculated from radius of the particle (=3 μm); L_{Au} is the thickness of gold (=100 nm); ρ_{Au} and ρ_{SiO2} are the mass density of the gold (19.3 g cm^{-3}) and bare silica particles (1.93 g cm^{-3}), respectively; V_{SiO2} is volume of silica particle; N_A is Avogadro's number; and M_{PAaH} is molecular weight of the PAaH-SH chain (=M_n).

RESULTS AND DISCUSSION

Preparation

The dithiobenzoate group at the pAaH chain-end can be cleaved to yield the corresponding thiol group.[27] Cleavage of the terminal dithiobenzoate group was confirmed by UV–visible absorption and ^{1}H NMR measurements. pAaH prepared by the RAFT process showed a UV–visible absorption at 299 nm because of the dithiobenzoate group at the chain end, which disappeared as a result of the cleavage (Supplementary Figure S1). Furthermore, cleavage was confirmed by ^{1}H NMR spectroscopy (Supplementary Figure S2). After the cleavage reaction, the peaks for the terminal phenyl protons at 7.6–8.3 p.p.m. disappeared, which suggested that quantitative cleavage of the terminal dithiobenzoate group in pAaH had taken place (Supplementary Figure S2).

The M_n and M_w/M_n values for pAaH and pAaH-SH, determined by GPC analysis using a phosphate buffer (pH 8, 50 mM) containing 9.1 vol % acetonitrile as eluent, were nearly the same (Supplementary Figure S3). The M_n values for pAaH and pAaH-SH were 4.93×10^4 and 4.96×10^4, respectively, and the M_w/M_n values for pAaH and pAaH-SH were 1.19 and 1.20, respectively. GPC data indicated an absence of bimodal coupling products that could be formed from the disulfide bond.

Table 1 Molecular weights and compositions of polymers

Polymer	*DP*	M_n*(GPC)* $\times$ 10^{-4}	M_w/M_n	*Flu content*[a] *(mol %)*
pAaH	220[b]	4.93	1.19	—
pAaH-SH	220[b]	4.96	1.20	—
P(AaH/Flu)	180[b]	3.50	1.05	0.2
P(AaH/Flu)-SH	180[b]	3.42	1.05	0.2
Conventional p(AaH/Flu)	8784[c]	182	1.42	0.1

Abbreviations: AaH, sodium 6-acrylamido hexanoate; DP, degree of polymerization; Flu, fluorescein; GPC, gel-permeation chromatography; M_n, number-average molecular weight; M_w/M_n, molecular weight distribution; SH, thiol.
[a]Determined by UV–visible absorption spectroscopy.
[b]Calculated from the conversion estimated by ^{1}H NMR.
[c]Calculated from GPC data.

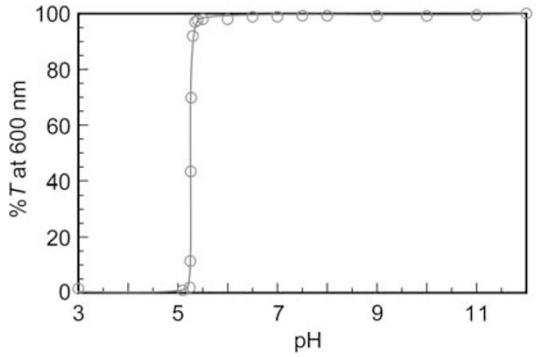

Figure 3 Percentage transmittance (%*T*) at 600 nm for aqueous solutions of pAaH as a function of solution pH. Polymer concentration=5.0 g l. A full color version of this figure is available at *Polymer Journal* online.

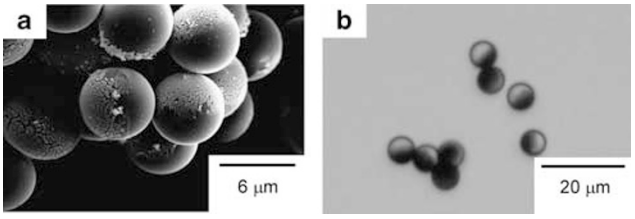

Figure 4 (**a**) s.e.m. and (**b**) optical microscope images of JPs. A full color version of this figure is available at *Polymer Journal* online.

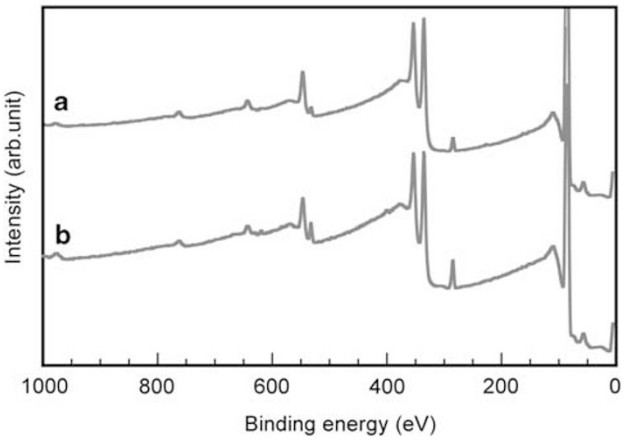

Figure 5 Survey XPS spectra for (**a**) the sputtered gold surface and (**b**) after immobilization of pAaH-SH on the sputtered gold surface.A full color version of this figure is available at *Polymer Journal* online.

Fluorescein-labeled pAaH (p(AaH/Flu)) was prepared via RAFT and conventional free radical polymerization. The Flu contents of p(AaH/Flu) and conventional p(AaH/Flu) were 0.2 and 0.1 mol %, respectively, as determined by UV–visible absorption spectroscopy. To prepare p(AaH/Flu)-SH, the dithioester group at the end of the p(AaH/Flu) polymer chain was cleaved in a manner similar to the preparation of pAaH-SH. Table 1 lists the molecular parameters of the polymers used in this study.

To investigate the pH-responsive behavior of pAaH in water, the pH dependence of %*T* at 600 nm was determined for an aqueous solution of pAaH (Figure 3). Above pH 5.2, the %*T* value was almost constant at 100% because the pendant carboxyl groups were deprotonated to form carboxylate anions; however, %*T* decreased sharply as the pH decreased from 5.5 to 5.2, reaching a minimum value of 0%. Interpolymer aggregation occurred below pH 5.2 owing to hydrophobic interactions among the pendant protonated carboxyl groups. These observations indicated that the transition from a water-soluble polymer to a precipitated interpolymer aggregate occurred within a narrow pH range.

Synthesis of JPs

Figure 4a shows a scanning electron microscope image of JPs. A boundary can be seen between the gold-covered and non-covered surface on the 6-μm SiO_2 particles. The gold adhered only to the side of the sphere facing the evaporation source, and it adhered sufficiently strongly that the evaporated gold could not be removed by sonication.

A water dispersion of JPs 6 μm in diameter (0.2 wt %) was dropped onto a slide glass, which was observed with an optical microscope with epi-illumination (Figure 4b). The gold-coated sides of the JPs appeared dark. Almost all of the particles showed a boundary between the gold-covered and the non-covered surface. At the bottom of the image, it may be observed that the gold-covered face of one of the particles is facing away toward the slide glass. The gold-covered surfaces of the JPs tend to associate with one another, presumably because of their hydrophobic nature.[28]

XPS measurements of pAaH-SH-grafted flat gold surface

To confirm the immobilization of pAaH-SH on the gold surface, we performed XPS experiments on pAaH-SH-grafted flat gold surfaces, rather than on pAaH-JPs. pAaH-SH was immobilized on the surface of a gold-sputtered cover glass. Figure 5a shows the survey-XPS spectrum for the sputtered gold surface. For the as-sputtered gold surface, a small amount of carbon was detected at 284.8 eV. The presence of sulfur and nitrogen was not confirmed by the narrow scan. In contrast, after immobilization of pAaH-SH on the sputtered gold surface, the peak height of carbon 1*s* at 284.8 eV increased as shown in Figure 5b.

Figure 6 shows the nitrogen and sulfur XPS spectra for the pAaH-SH-grafted gold surface. The presence of nitrogen and sulfur was confirmed. Table 2 shows the binding energies, obtained by XPS analysis, of pAaH-SH and the pAaH-SH-grafted gold surface. The photoelectron peak of the sulfur $2p^{1/2}$ energy level for pAaH-SH was observed at 163.9 eV, corresponding to unbound free thiol groups. The sulfur peak for the pAaH-SH-grafted gold surface was observed at 161.4 eV, which is characteristic of thiolate binding to a gold surface.[29] This observation suggests that pAaH-SH was immobilized on the gold surface; therefore, it was concluded that pAaH-SH could be immobilized on the gold surface of JPs.

Water contact angle measurements for the pAaH-grafted flat gold surface

We wished to confirm that the pH-responsive association behavior of pAaH-JPs could be attributed to changes in polarity on the pAaH-

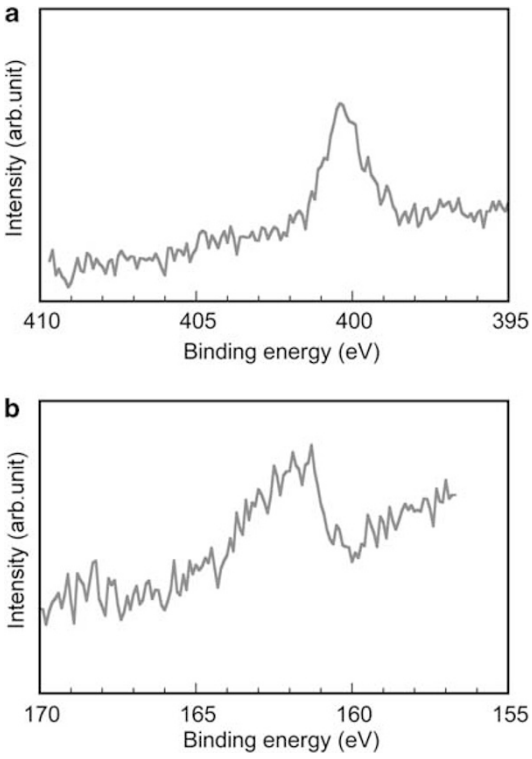

Figure 6 (**a**) Nitrogen- and (**b**) sulfur-XPS spectra for the pAaH-SH-grafted gold surface. A full color version of this figure is available at *Polymer Journal* online.

Table 2 Binding energies for pAaH-SH and pAaH-SH-grafted gold surface, estimated by XPS

	C (eV)	*S (eV)*	*N (eV)*	*Au (eV)*
pAaH-SH	284.8	163.9	400.7	—
pAaH-SH-grafted gold surface	284.8	161.4	400.4	84.0

Abbreviations: AaH, sodium 6-acrylamido hexanoate; Au, gold; C, carbon; N, nitrogen; S, sulfur; SH, thiol.

grafted gold surface. However, it was difficult to measure the surface micropolarity on the gold surface of pAaH-JPs because of the small area of the gold surface. Therefore, we instead confirmed the existence of pH-responsive changes in the surface polarity of a pAaH-SH-grafted flat gold surface. pAaH-SH was immobilized on the gold-sputtered slide glass surface, and pH-responsive polarity changes in the pAaH-grafted gold surface were evaluated using contact angle measurements.

Contact angle measurements were performed on gold-sputtered cover glasses and on pAaH-SH-immobilized gold surfaces. The pAaH-SH-grafted gold surfaces were treated by soaking in aqueous solutions of pH 3 and 10 for 24 h, and then washed with pure water. Figure 7 shows pure water droplets on the gold surface and the pAaH-SH-grafted gold surface treated with water at pH 3 and 10. The contact angle with pure water on the gold surface before immobilization of pAaH-SH was 77.7° (Figure 7a), whereas the contact angles with pure water on the pAaH-SH-grafted gold surface treated with aqueous solutions of pH 3 and 10 were 85.0° and 53.8°, respectively (Figures 7b and c). The pAaH-SH-grafted gold surface treated with an aqueous solution of pH 3 became more hydrophobic than the original gold-sputtered surface, because the grafted pAaH-SH chains became

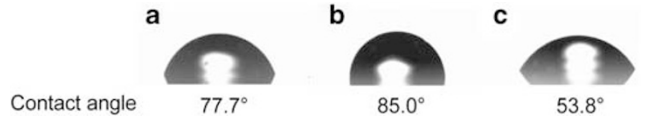

Figure 7 Water contact angles of the gold surface (**a**) before immobilization of pAaH-SH; and after immobilization of pAaH-SH at (**b**) pH 3 and (**c**) pH 10.

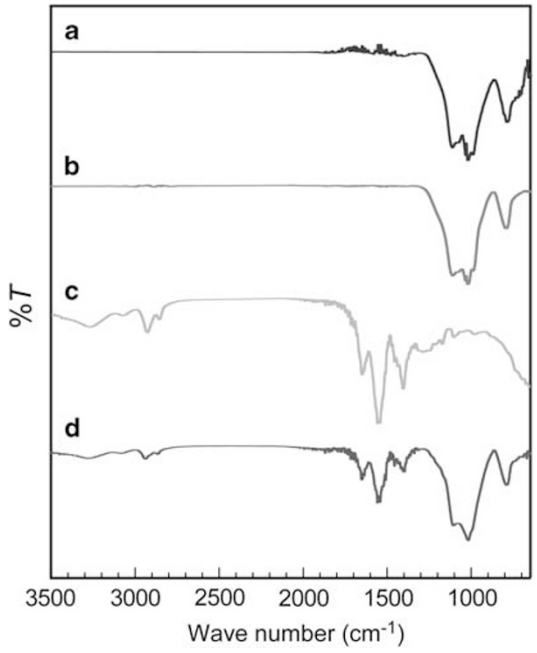

Figure 8 ATR-FTIR spectra for (**a**) untreated SiO_2 particles, (**b**) JPs, (**c**) pAaH-SH, and (**d**) pAaH-JPs in the 650–3500 cm^{-1} region. A full color version of this figure is available at *Polymer Journal* online.

hydrophobic owing to protonation of the pendant carboxyl groups. In contrast, the contact angle on the pAaH-SH-grafted gold surface treated with a pH 10 aqueous solution was smaller than that of the original gold-sputtered surface and the pAaH-SH grafted-gold surface treated with a pH 3 aqueous solution, because the pendant carboxyl groups in pAaH-SH were deprotonated to form carboxylate anions. These observations suggested that the polarity of the pAaH-SH-grafted gold surface might be controlled by varying the pH.

ATR-FTIR measurements for pAaH-JPs

Immobilization of pAaH-SH on the gold surface of JPs was confirmed by ATR-FTIR measurements. Figure 8 shows ATR-FTIR spectra of untreated SiO_2 particles, JPs, pAaH, and pAaH-JPs. The ATR-FTIR spectrum of JPs (Figure 8a) was almost the same as that of untreated SiO_2 particles (Figure 8b). In the spectrum of hybrid pAaH-JPs (Figure 8d), absorption peaks characteristic of pAaH chains (Figure 8c) were observed at 3 266 (amide, N-H), 1 547 (amide, C=O) and 2 937 cm^{-1} (C-H), indicating that the immobilization of pAaH on the gold surface of the JPs was successfully achieved.

TGA measurements for pAaH-JPs

The TGA curve for the pAaH-JP is given in Figure 9. TGA measurements on the pAaH-JPs indicated that pAaH-SH decomposed in the temperature range 200–420 °C. The weight loss of the pAaH-JP was 0.45%. Thus, the surface density of the pAaH-SH chain can be calculated from equation (1) to be 0.28 chains per nm^2. Fukuda

et al.[30] reported a gold nanoparticle coated with poly(methyl methacrylate) prepared by surface-initiated atom transfer radical polymerization of methyl methacrylate with an initiator-coated gold nanoparticle. The graft density on the gold surface is nearly constant, independent of the molecular weight of poly(methyl methacrylate), and estimated to be 0.3 chains/nm^2.

Observation of fluorescein-labeled pAaH-JPs

We confirmed the immobilization of pAaH-SH on the gold surface of JPs using a fluorescence microscopy technique. Fluorescein-labeled pAaH-SH (p(AaH/Flu)-SH) was mixed with JPs in water. The p(AaH/Flu)-SH-grafted JPs (p(AaH/Flu)-JPs) were washed with pure water several times and observed using optical and fluorescence microscopes. Figure 10 shows optical microscope, fluorescence microscope and overlaid images of p(AaH/Flu)-JPs. The sides of the JPs coated with gold appeared dark in the optical microscope image (Figure 10a). In the fluorescence microscope (Figure 10b) and overlaid images (Figure 10c), fluorescence can be observed from the gold-coated sides of the JPs. This observation indicates that pAaH-SH can be immobilized only on the gold surface of the JPs.

Furthermore, we wished to confirm that pAaH-SH does not adsorb onto the SiO_2 surface during the preparation of pAaH-JPs. To examine the adsorption of pAaH-SH onto the SiO_2 surface, p(AaH/Flu)-SH was mixed with untreated SiO_2 particles in water. The SiO_2 particles were washed several times with pure water and observed with optical (Figure 10d) and fluorescence microscopy techniques (Figure 10e). Fluorescence was not observed from the SiO_2 particles treated with p(AaH/Flu)-SH, which indicated that p(AaH/Flu)-SH was not adsorbed to the SiO_2 surface.

Fluorescein-labeled pAaH prepared via conventional free radical polymerization (conventional p(AaH/Flu)) was mixed with JPs in water and washed several times with pure water. Fluorescence was not observed from these particles (Figures 10f and g). These observations indicated that only thiol-terminated polymer chains can be immobilized on the gold surface of JPs.

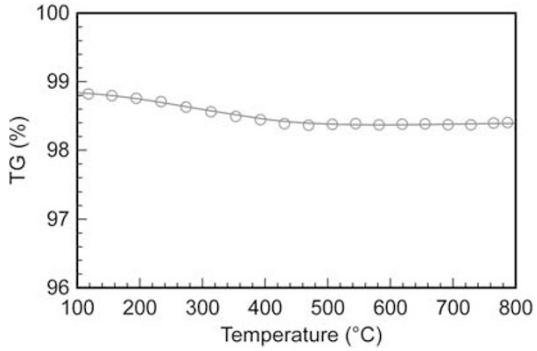

Figure 9 TGA curve for the pAaH-JP measured at a heating rate of 5 °C min^{-1} under nitrogen. A full color version of this figure is available at *Polymer Journal* online.

pH-responsive flocculation and dispersion behavior of pAaH-JPs

The pH-responsive flocculation and dispersion behavior of hybrid pAaH-JPs in water was studied using optical microscopy. Figure 11 shows optical micrographs of pAaH-JPs in water at pH 3 and 10. At pH 3, flocculation of the pAaH-JPs was observed, owing to hydrophobic interactions of the protonated pAaH chains grafted onto the gold surface (Figure 11a). Owing to the hydrophobicity of the pendent hexanoic acid groups in pAaH, the wettability of the gold surface of the pAaH-JPs decreased at pH 3. From the analogy of the amphiphilic molecules, pAaH-JPs may be able to form ordered assemblies like micelles at pH 3. However, Figure 11a shows only simple flocculation of pAaH-JPs. The motion of the JPs cannot obey ordinary Brownian motion in water. The density of JPs is much higher than that of water because the density of bare SiO_2 particles is 1.93 g cm^{-3}, and, moreover, JPs were coated with gold (ρ_{Au}=19.3 g cm^{-3}) at one side.

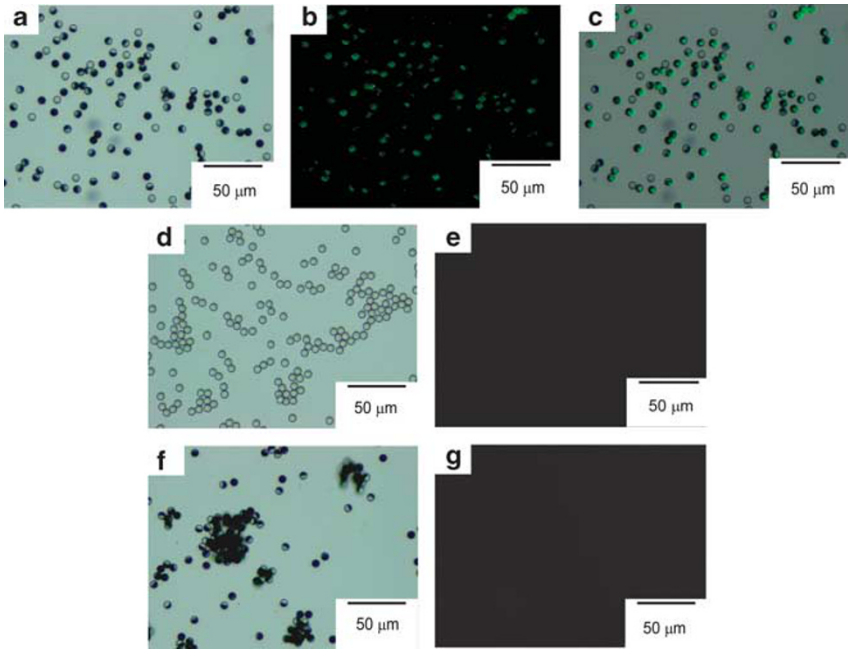

Figure 10 (**a**) Optical and (**b**) fluorescence microscopy images of p(AaH/Flu)-JPs, and (**c**) overlaid image of (**a**) and (**b**). (**d**) Optical and (**e**) fluorescence microscope images of a mixture of p(AaH/Flu)-SH and untreated SiO_2 particles. (**f**) Optical and (**g**) fluorescence microscope images of a mixture of conventional p(AaH/Flu), without the terminal SH group, and JPs.

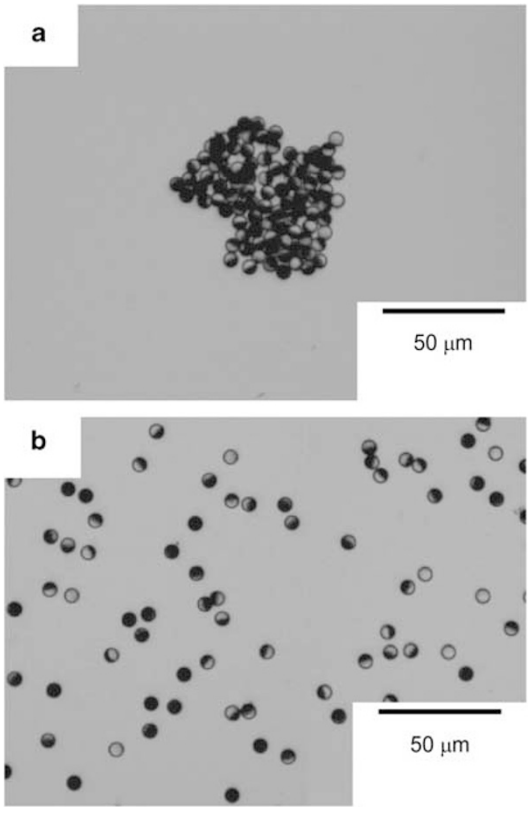

Figure 11 Optical micrographs of pAaH-JPs in water at (**a**) pH 3 and (**b**) pH 10. A full color version of this figure is available at *Polymer Journal* online.

Aqueous NaOH was added to the pH 3 aqueous suspension of pAaH-JPs to adjust the pH from 3 to 10, and the suspension was mixed with a vortex mixer for 1 min (Figure 11b). The particles were dispersed separately because of electrostatic repulsion between the negatively charged pendant hexanoate groups in the pAaH graft chains. It was concluded that at pH 10, the grafted pAaH chains became hydrophilic polyanions owing to deprotonation of the pendant hexanoate groups. These observations indicate that the flocculation and dispersion behavior of pAaH-JPs in water can be controlled by varying the solution pH.

CONCLUSIONS

pH-responsive pAaH, possessing a thiol group at the end of the polymer chain, was successfully synthesized via RAFT radical polymerization. pH-responsive solubility changes of pAaH in water were confirmed by %*T* measurement. We also prepared JPs composed of SiO_2 particles 6 μm in diameter half-coated with gold by a vapor deposition method. The successful synthesis of these size-controlled asymmetric particles was confirmed by scanning electron microscopy and optical microscopy observations. pAaH-SH was immobilized on the gold surface of JPs by mixing the two materials in water, as confirmed by XPS, ATR-FTIR and fluorescence microscopy observations using fluorescein-labeled pAaH-SH. The flocculation and dispersion behavior of hybrid pAaH-JPs in water could be controlled by varying the solution pH. At pH 10, pAaH-JPs were dispersed in water because the pAaH graft chains were hydrophilic owing to ionization of the pendant carboxyl groups; in contrast, at pH 3, flocculation of pAaH-JPs was observed because the pAaH chains became hydrophobic owing to protonation of the pendant carboxyl groups. The results of this study may be applied to the development of functional emulsifying agents with stimuli-responsive stabilization behavior.

ACKNOWLEDGEMENTS

T Shiono is thanked for his experimental support. This work was supported by a Grant-in-Aid (No. 21106518) for Scientific Research in Innovative Areas, 'Molecular Soft-Interface Science,' from the Ministry of Education, Culture, Sports, Science and Technology of Japan.

1 Paunov, V. N. & Cayre, O. J. Supraparticles and 'Janus' particles fabricated by replication of particle monolayers at liquid surfaces using a gel trapping technique. *Adv. Mater.* **16,** 788–791 (2004).
2 Saito, N., Kagari, Y. & Okubo, M. Effect of colloidal stabilizer on the shape of polystyrene/poly(methyl methacrylate) composite particles prepared in aqueous medium by the solvent evaporation method. *Langmuir* **22,** 9397–9402 (2006).
3 Higuchi, T., Tajima, A., Yabu, H. & Shimomura, M. Spontaneous formation of polymer nanoparticles with inner micro-phase separation structures. *Soft Matter* **4,** 1302–1305 (2008).
4 Casagrande, C. & Veyssié, M. Janus beads-realization and 1st observation of interfacial properties. *C. R. Acad. Sci. Ser. II* **306,** 1423–1425 (1998).
5 Yoshida, M. & Lahann, J. Smart nanomaterials. *ACS Nano* **2,** 1101–1107 (2008).
6 Glotzer, S. C. & Solomon, M. J. Anisotropy of building blocks and their assembly into complex structures. *Nat. Mater.* **6,** 557–562 (2007).
7 Perro, A., Reculusa, S., Ravaine, S., Bourgeat-Lami, E. & Duguet, E. Design and synthesis of Janus micro- and nanoparticles. *J. Mater. Chem.* **15,** 3745–3760 (2005).
8 Fujimoto, K., Nakahama, K., Shidara, M. & Kawaguchi, H. Preparation of unsymmetrical microspheres at the interfaces. *Langmuir* **15,** 4630–4635 (1999).
9 Walther, A. & Müller, A. H. E. Janus particles. *Soft Matter* **4,** 663–668 (2008).
10 Hong, L., Cacciuto, A., Luijten, E. & Granick, S. Clusters of charged janus spheres. *Nano Lett.* **6,** 2510–2514 (2006).
11 Hong, L., Cacciuto, A., Luijten, E. & Granick, S. Clusters of amphiphilic colloidal spheres. *Langmuir* **24,** 621–625 (2008).
12 Lattuada, M. & Hatton, T. A. Preparation and controlled self-assembly of Janus magnetic nanoparticles. *J. Am. Chem. Soc.* **129,** 12878–12889 (2007).
13 Takahara, Y. K., Ikeda, S., Ishino, S., Tachi, K., Ikeue, K., Sakata, T., Hasegawa, T., Mori, H., Matsumura, M. & Ohtani, B. Asymmetrically modified silica particles: a simple particulate surfactant for stabilization of oil droplets in water. *J. Am. Chem. Soc.* **127,** 6271–6275 (2005).
14 Nisisako, T., Torii, T., Takahashi, T. & Takizawa, Y. Synthesis of monodisperse bicolored Janus particles with electrical anisotropy using a microfluidic co-flow system. *Adv. Mater.* **18,** 1152–1156 (2006).
15 Suci, P. A., Kang, S., Young, M. & Douglas, T. A streptavidin–protein cage Janus particle for polarized targeting and modular functionalization. *J. Am. Chem. Soc.* **131,** 9164–9165 (2009).
16 Tanaka, T., Okayama, M., Kitayama, Y., Kagawa, Y. & Okubo, M. Preparation of 'mushroom-like' Janus particles by site-selective surface-initiated atom transfer radical polymerization in aqueous dispersed systems. *Langmuir* **26,** 7843–7847 (2010).
17 Ye, S. & Carroll, R. L. Design and fabrication of bimetallic colloidal 'Janus' particles. *ACS Appl. Mater. Interfaces* **2,** 616–620 (2010).
18 Feng, X., Taton, D., Ibarboure, E., Chaikof, E. L. & Gnanou, Y. Janus-type dendrimer-like poly(ethylene oxide)s. *J. Am. Chem. Soc.* **130,** 11662–11676 (2008).
19 Love, J. C., Gates, B. D., Wolfe, D. B., Paul, K. E. & Whitesides, G. M. Fabrication and wetting properties of metallic half-shells with submicron diameters. *Nano Lett.* **2,** 891–894 (2002).
20 Kato, M., Kamigaito, M., Sawamoto, M. & Higashimura, T. Polymerization of methyl methacrylate with the carbon tetrachloride/dichlorotris- (triphenylphosphine)ruthenium(II)/methylaluminum bis(2,6-di-*tert*-butylphenoxide) initiating system: possibility of living radical polymerization. *Macromolecules* **28,** 1721–1723 (1995).
21 Chiefari, J., Chong, Y. K., Ercole, F., Krstina, J., Jeffery, J., Le, T. P. T., Mayadunne, R. T. A., Meijs, G. F., Moad, C. L., Moad, G., Rizzardo, E. & Thang, S. H. Living free-radical polymerization by reversible addition-fragmentation chain transfer: the RAFT process. *Macromolecules* **31,** 5559–5562 (1998).
22 Zelikin, A. N., Such, G. K., Postma, A. & Caruso, F. Poly(vinylpyrrolidone) for bioconjugation and surface ligand immobilization. *Biomacromolecules* **8,** 2950–2953 (2007).
23 Qiu, X.- P. & Winnik, F. M. Facile and efficient one-pot transformation of RAFT polymer end groups via a mild aminolysis/michael addition sequence. *Macromol. Rapid Commun.* **27,** 1648–1653 (2006).
24 Shibaev, V. P., Platé, N. A. & Freidzon, Y. S. Thermotropic liquid crystalline polymers. I. Cholesterol-containing polymers and copolymers. *J. Polym. Sci. Polym. Chem. Ed.* **17,** 1655–1670 (1979).
25 Mitsukami, Y., Donovan, M. S., Lowe, A. B. & McCormick, C. L. Water-soluble polymers. 81. direct synthesis of hydrophilic styrenic-based homopolymers and

block copolymers in aqueous solution via RAFT. *Macromolecules* **34,** 2248–2256 (2001).
26 Takei, H. & Shimizu, N. Gradient sensitive microscopic probes prepared by gold evaporation and chemisorption on latex spheres. *Langmuir* **13,** 1865–1868 (1997).
27 Nakayama, M. & Okano, T. Polymer terminal group effects on properties of thermoresponsive polymeric micelles with controlled outer-shell chain lengths. *Biomacromolecules* **6,** 2320–2327 (2005).
28 Butt, H. J-., Graf, K. & Kappl, M. *Physics and Chemistry of Interfaces* (Wiley-VCH: Veriag GmbH & Co, KgaA, Weinheim, Germany, 2006).
29 Kanoh, N., Kyo, M., Inamori, K., Ando, A., Asami, A., Nakao, A. & Osada, H. SPR imaging of photo-cross-linked small-molecule arrays on gold. *Anal. Chem.* **78,** 2226–2230 (2006).
30 Ohno, K., Koh, K., Tsujii, Y. & Fukuda, T. Synthesis of gold nanoparticles coated with well-defined, high-density Polymer brushes by surface-initiated living radical polymerization. *Macromolecules* **35,** 8989–8993 (2002).

Supplementary Information accompanies the paper on Polymer Journal website (http://www.nature.com/pj)